

## **LULC impacts on NDVI and LST: A case study on Jashore District, Bangladesh**

### **Abstract**

Studies on land use and land cover (LULC) changes and subsequent effects on environment are not satisfactory in Bangladesh because of the lack of geospatial data and time-series information. By using the open-source Landsat data coupled with GIS technology and other ancillary data, the main purpose of this study is to analyze the dynamic changes in LULC in Jashore District of Bangladesh over a 20-year period between 2002 and 2022. Including pre-classification and post-classification identification scenarios, Normalized Difference Vegetation Index (NDVI) analysis was employed to examine the vegetation changes over the period. The findings of this present study indicate notable changes with an increase of 20.77% in urban areas and 14.53% in bare soil. Additionally, there has been a decline of 2.93% in water bodies and 32.37% in vegetation land cover. Accuracy evaluations of supporting the land use classification's trustworthiness include Kappa statistics of 0.80 for the year 2022 and 0.65 for the year 2002. A decrease in land surface temperature (LST) in Jashore District over 20 years from 2002 to 2022 has been reported in this study. Although the proportion of vegetation cover has been reduced in 2022, we found a negative correlation between LST and NDVI. Along with LULC, the LST is influenced by many other atmospheric and ecological parameters, which could also be affected by recent global climate change. Furthermore, NDVI is dependent on vegetation canopy type, color and density, which could also affect the relationship with LST. The findings of this study provide insightful

information to ecologists, environmentalists, urban planners, and lawmakers for developing sustainable land management plans and environmental conservation initiatives.

**Keywords:** LULC; Kappa statistics; LST; NDVI; Jashore district.

## **Introduction**

The cities in Bangladesh experience one of the fastest urbanization rates in the world over the past few decades (Faisal et al. 2021). Rapid population growth and the migration of people to urban areas cause informal settlements, uncontrolled expansion of slums, fast-spreading disease (Moore et al. 2003), pervasive urban poverty (Grant 2010), traffic jams (Islam and Ahmed 2011), waterlogging, environmental pollution and degradation (Kafy et al. 2020) and other socioeconomic issues (Gómez et al. 2020). Mostly the uncontrolled population growth and unplanned urbanization hinder sustainable development of the cities in Bangladesh (Kafy et al. 2021). For the sustainable land use, distribution and management of environmental and ecological resources, it is essential to consider the changes in urban land use and land cover (LULC). Land use refers to how humans utilize lands for purposes like agriculture, industry, or recreation (Rawat and Kumar 2015), whereas the land cover relates to the physical characteristics of the Earth's surface, such as agricultural lands, woodlands, water bodies, urban areas and natural vegetation (Audah et al. 2021; Mishaa et al. 2021). Land use and land cover (LULC) is a critical component because of its potential environmental impact on natural resource management (Iqbal and Khan 2014; Kantakumar and Neelamsetti 2015; Lin et al. 2015). It may contribute to global environmental change through the interaction with biodiversity, biogeochemical cycles, climatic systems, biological processes, and human activities (Agarwal et al. 2001; Lopez et al. 2001). At local, regional, and global dimensions, the changes in LULC impact the equilibrium of energy, water, agricultural production, and geochemical exchanges.

Thus, comprehensive knowledge of LULC changes is crucial for the sustainable management of land, allocation of resources, and preservation of the environment (Vescovi et al. 2002).

Geospatial technology like satellite-based remote sensing (RS) and geographic information system (GIS) has revolutionized the research area of LULC by providing detailed qualitative and quantitative information for observing and recording LULC changes at a particular time and spatial location (Collins et al. 1996; Gopal et al. 1996; Mamun 2013). Considering that the classification of LULC is an ongoing and dynamic process, it is essential to do continuous research on LULC changes and their impacts on both the society and the environment (López et al. 2001; Mondal et al. 2016). All developed nations and majority of developing nations have access to current comprehensive LULC data, which enables them to monitor changes in their landforms. Hence, they are ready to face new environmental challenges and issues in advance. However, Bangladesh, as a developing nation, is not under continuous monitoring of LULC changes to overcome current challenges for the establishment of sustainable ecosystems. In the context of Bangladesh, various environmental challenges such as soil and water pollution, soil quality degradation, soil erosion, loss of minimum area of vegetation, and loss of biodiversity have been exacerbated mostly because of the rapid expansion of population and inadequate urban planning (Xu et al. 2020). Therefore, it is crucial to research the amount of farmed land, vegetation, water features, and wet/lowland areas that are lost to urban areas.

Land surface temperature (LST) is one of the most important parameters of surface-atmosphere interactions and climate change, which significantly alters seasonal vegetation phenology and in turn affects the energy balance at global and regional scale. Thermal RS techniques can measure the upward long-wave radiation from the land surface under clear sky and the data are used to retrieve the spatially distributed LSTs. LST is strongly influenced by

landscape features as the features change the thermal characteristics of the surface greatly. The methods of anthropogenic heat discharge due to energy consumption cause increase in LST. In contrast, the vegetation and water surfaces in a landscape reduce the LST through evapotranspiration (Kumar et al. 2012). Thus, the lowest LSTs are usually found in dense vegetative areas. However, the LST is dependent on time, place and types and distributions of vegetation (Yuan and Bauer 2007). As a victim of climate change, Bangladesh is expecting a gradual increase in LST (Mondal and Wasimi 2004). Multiple research projects have confirmed a significant correlation between LULC and land surface temperature (LST). Researchers have found that the increase in LST is particularly influenced by changes in LULC, particularly in metropolitan regions (Weng et al. 2004; Kumar and Shekhar 2015; Fan et al. 2017; Pal and Ziaul 2017). RS and GIS technology are significant contemporary techniques used to identify LULC and extract LST (Choudhury et al. 2019).

For Bangladesh perspective, previous studies on LULC change and its impact on cities are available (e.g., Uddin and Gurung 2008; Dewan and Yamaguchi 2009a, 2009b; Islam and Ahmed 2011; Mamun et al. 2013; Haque and Basak 2017; Islam and Ma 2018; Kafy et al. 2020; Xu et al. 2020; Morshed et al. 2021; Morshed et al. 2023). However, the previously available studies on changes in LULC mostly cover the study sites as the capital city Dhaka (e.g., Ahmed and Bramley 2015; Pramanik and Stathakis 2015; Hossain and Rahman 2022), the most commercial city Chittagong (Hassan and Nazem 2016) and other big cities like Rajshahi (Hassan 2017; Kafy et al. 2019), Sylhet, Rangpur, Barishal (Hassan 2017), Khulna (Ahmed 2011; Hassan 2017), and Sunamganj (Haque and Basak 2017). Having access to current and comprehensive LULC data allows many developing nations to keep track of changes to their landforms. This is not the case for developing nations like Bangladesh. The LULC structure is complicated and

must be monitored periodically for better understanding of future urban growth pattern (Al-Darwish et al. 2018; Feng et al. 2018). Investigating the loss of farmed land that has been moved to urban areas as well as the alterations to vegetation, water bodies, and wet/lowlands is therefore imperative. A recent study has reported on future potential intra-urban LULC growth patterns of a developing city Jashore in Bangladesh up to the year 2050 (Morshed et al. 2023). However, as a first attempt, this present study is accomplished in Jashore District for analyzing the patterns of LULC changes and the effects of those changes on LST through the creation of the Normalized Difference Vegetation Index (NDVI) and spatiotemporal change maps by using GIS and RS technologies. It would be a great step towards strategic planning for sustainable urban development of that city (Maarseveen et al. 2018). NDVI is a metric which is employed to measure temporal variations in vegetative patterns. Therefore, the specific objectives of the present study are to identify (i) the significant changes in LULC, LST and NDVI over a period of 20 years by using 2002 as the reference year and (ii) the relationship analysis between LST and NDVI. The findings of this study are expected helping the national policymakers to set strategies for controlling urban growth and environmental changes in future.

## **Methodology**

### **Study Area**

Jashore District, situated in the southwestern region of Bangladesh, has a tropical monsoon climate. Geographically, it is situated within the latitudes 23°0'N to 23°22'N and the longitudes 88°55'E to 89°15'E (Fig. 1). Geographically, the district is next to Narail in the northeast, Magura in the northwest, Khulna in the south, and the Republic of India, particularly the state of West Bengal, in the west. The district has a total land area of 2545.32 square kilometers. It is

surrounded by a multitude of water bodies, including the Bhairab, Teka, Hari, Sree, Aparbhadra, Harihar, Haribhadra, Chitra, Betna, Kopotakkho, and Mukteshwari rivers.

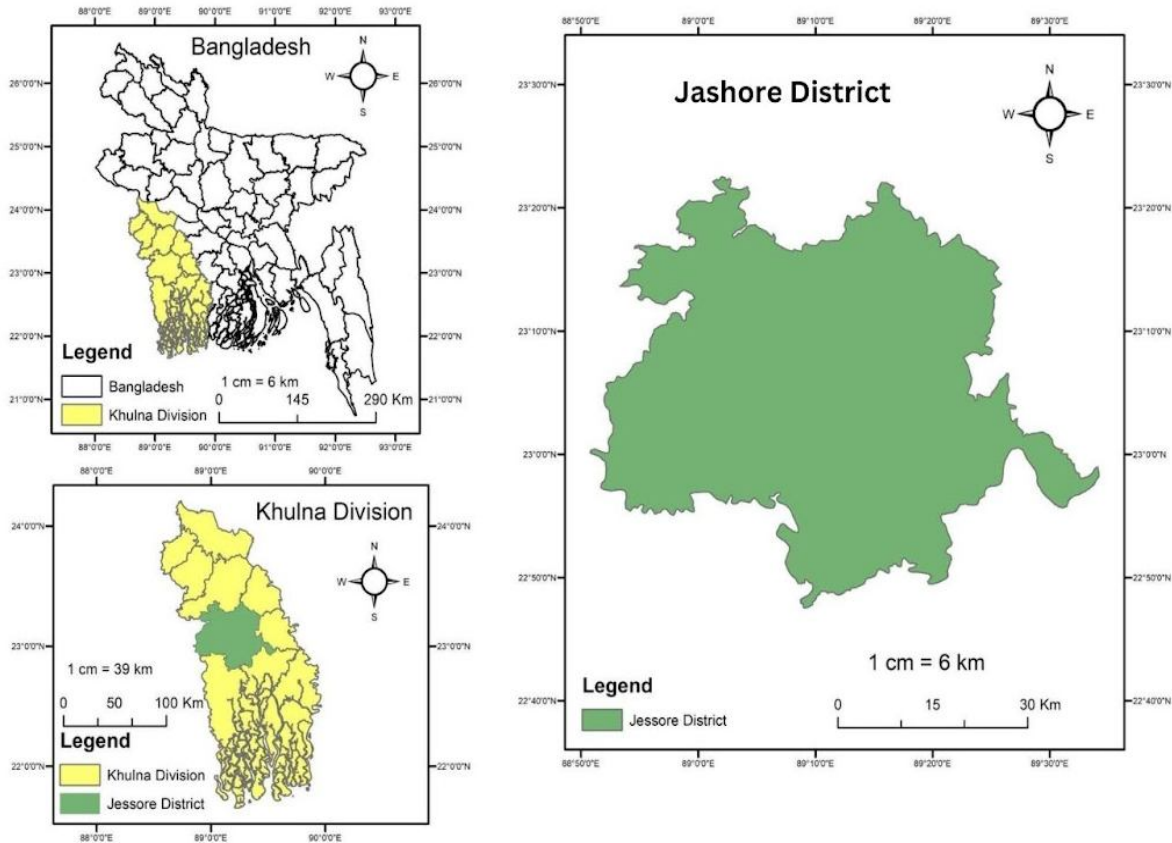


Figure 1 Study area, the Jashore District under Khulna Division in Bangladesh.

## Data Collection

The present analysis is dependent on secondary data and incorporates a diverse range of geographic and non-spatial data sources. The geographic and temporal data employed in this work were the latest high-resolution satellite pictures, namely Landsat ETM+ 30m (year 2002) and OLI-TIRS 30m (year 2022), which have a row/path value of 44/138 with a resolution of 30 meters. The photos were obtained from the publicly accessible Landsat imaging services accessible at <https://earthexplorer.usgs.gov>. Table 1 presents the characteristics of the Landsat

data. Cloud-free and undesired shade-free photos were given priority during the image selection process. To avoid clouds and expecting minimal variation in the period of capturing images, the study mostly used imagery data from the winter season (Uddin and Gurung 2008). The satellite images were georeferenced using the World Geodetic System (WGS) 84 coordinate system and the Universal Transverse Mercator (UTM) map projection in Zone 46 N datum. The shape file for the Jashore District was sourced from the Bangladesh Water Development Board (BWDB). The base maps of Jashore City were obtained from published papers by the Geological Survey of Bangladesh (GSB) for reference.

Table 1: Information on Landsat Satellite data used.

Satellite	Sensor	Row / Path	Date	Resolution	Band information	Wavelength (m)	Data source
Landsat-8	OLI-TIRS	44/138	2022-02-07	30	B2 (Blue)	0.45-0.51	<a href="https://earthexplorer.usgs.gov/">https://earthexplorer.usgs.gov/</a>
					B3 (Green)	0.53-0.59	
					B4 (Red)	0.64-0.67	
					B5 (NIR)	0.85-0.88	
					B8 (Panchromatic)	0.50-0.68	
Landsat-7	ETM+	44/138	2002-02-24	30	B1 (Blue)	0.45-0.51	<a href="https://earthexplorer.usgs.gov/">https://earthexplorer.usgs.gov/</a>
					B2 (Green)	0.52-0.60	
					B3 (Red)	0.63-0.69	
					B4 (NIR)	0.77-0.90	
					B8 (Panchromatic)	0.50-0.68	

### Pre-processing of Data

The processes of stacking the Landsat imagery, combining them into multiband composite views, and focusing on the research region were imperative to optimize the quality and efficiency of the subsequent analyses. Using ArcGIS 10.8, the layer stacking process was carried out effectively, reducing the required bands into a small layer for the photos to be examined. To precisely align and synchronize the imageries used in this study, image registration was essential. In this case, the 2002 Landsat-7 imagery was registered against the Landsat-8 image from 2022

(path 138, row 44) as the reference. After registration, the photos were put through several pre-processing steps to remove any possible distortions or irregularities. The most important procedure among the pre-processing steps was atmospheric adjustment, which made sure that the accuracy of the data was not harmed by interference from gasses and other atmospheric particles. Furthermore, radiometric adjustments were applied to account for any anomalies or atmospheric noise, specifically tackling cloud-related issues. The thorough pre-processing procedures established a strong basis for the ensuing picture analysis, ensuring precision and reliability in the results.

### **Method of classification and change detection of LULC**

The LULC map was classified using the maximum likelihood method of the Image Classification tool in ArcGIS 10.8, which is a supervised classification procedure. The land use categorization has been based on the bands 1-4 and 8 of the Landsat-7 ETM+ aerial photography. Furthermore, the classification of land use has been based on bands 2-4 and band-8 of the Landsat-8 OLI images. To generate the LULC maps, the image analyzer tool inside the ArcGIS 10.8 program was utilized to stack all the bands. The training sample management tool, with randomly chosen substantial quantity of training samples, was thereafter employed to determine the pixel signature. The flow chart in Figure 2 depicts the complete procedure of land use classification.

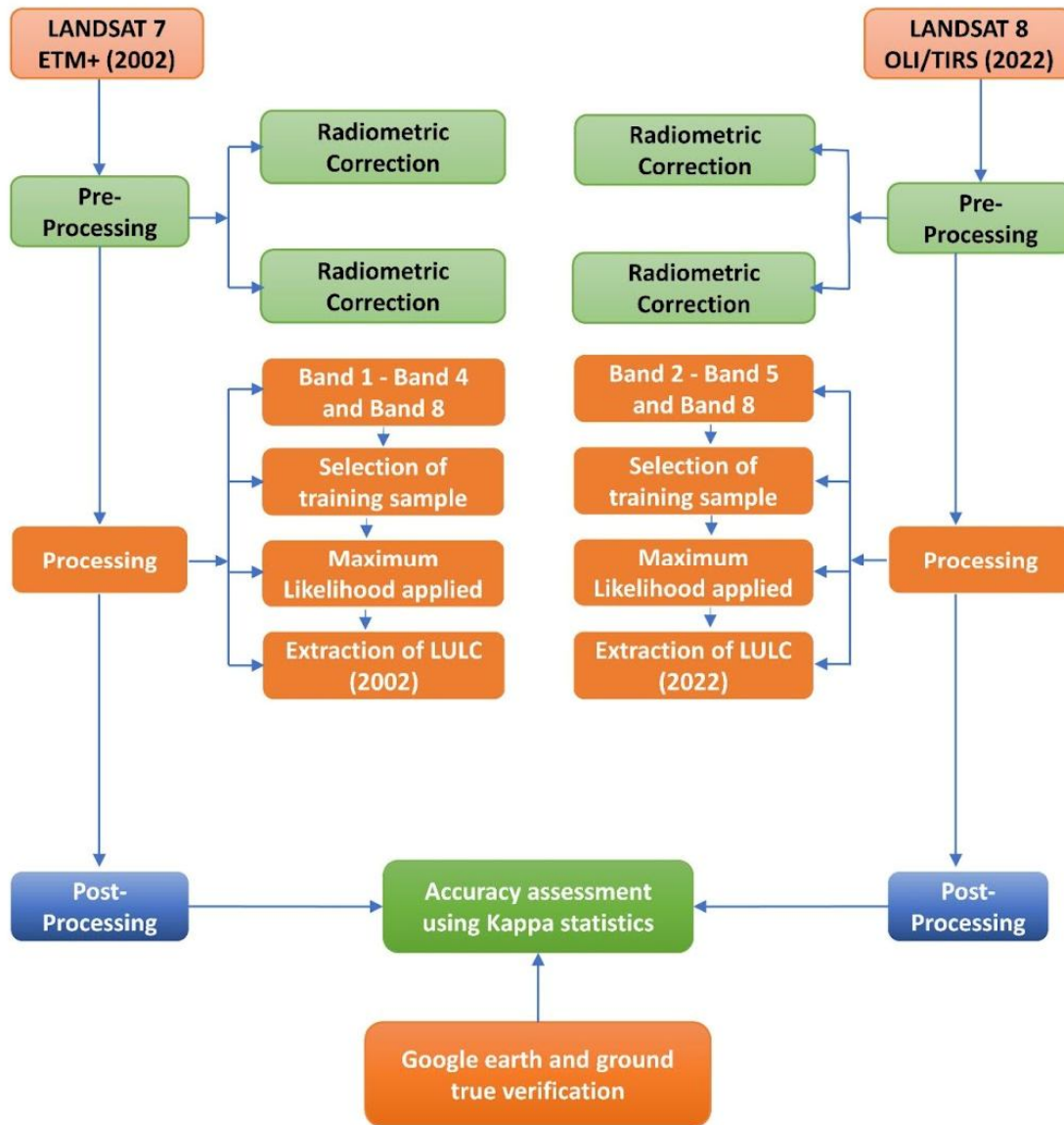


Figure 2 Procedures for LULC classification.

### Method of accuracy assessment of LULC maps

The accuracy assessment is necessary for both pre- and post-classified imagery. The confusion matrix or error matrix has been used to evaluate the study's reliability. The following equations were used to conduct the accuracy assessment in this study (Das et al. 2021):

Overall Accuracy =

$$\frac{\text{Total Number of Correctly Classified pixels(Diagonal)}}{\text{Total Number of Reference pixels}} \times 100 \dots \dots \dots (1)$$

$$\text{User Accuracy} = \frac{\text{Number of Correctly Classified pixels in each category}}{\text{Total Number of Classified Pixel in that category(The Row Total)}} \times 100 \dots \dots \dots (2)$$

Producer Accuracy =

$$\frac{\text{Number of Correctly Classified pixels in each category}}{\text{Total Number of Reference Pixels in that category(The Column Total)}} \times 100 \dots \dots \dots (3)$$

Kappa Coefficient (T) =

$$\frac{((TS \times TCS) - \Sigma(\text{Column Total} \times \text{Row Total}))}{(TS \wedge 2 - \Sigma(\text{Column Total} \times \text{Row Total}))} \times 100 \dots \dots \dots (4)$$

### Method for calculation of NDVI

The present study has shown a correlation between the Normalized Difference Vegetation Index (NDVI) and Land Surface Temperature (LST). The NDVI is a vegetation index that measures the variation in reflectance characteristics across wavelengths in the near-infrared and red ranges. The quantity is determined by dividing the total of these two reflectance values. The NDVI extraction has been successfully achieved using the methodology provided by (Townshend and Justice 1986).

$$NDVI = \left( \frac{NIR - RED}{NIR + RED} \right) \dots \dots \dots (5)$$

where, the acronym NIR denotes the near Infrared band, while RED designates the red band. NDVI was extracted using Landsat ETM+ band 3 and band 5, along with Landsat OLI band 4 and band 5. Numerical NDVI values span from -1 (negative) to +1 (positive). NDVI readings that are negative provide evidence of water, whereas values that are positive suggest the existence of vegetation.

**Method of LST from the thermal band**

The thermal bands of Landsat-7 ETM+ (band 6) and Landsat-8 OLI (band 10) were used to calculate the ground surface temperature for the month of February, which correspond to the winter season. Yet, the approach of obtaining LST from Landsat ETM+ and Landsat OLI varies somewhat in terms of computing spectral radiance ( $L\lambda$ ). The methodologies for obtaining LST have been well explained in several research papers (Asgarian et al. 2014; Govind and Ramesh 2019). The sequential procedure of obtaining LST from Landsat ETM+ and Landsat OLI images is depicted in Figure 3. Below is the detailed, step-by-step technique for calculating LST:

Step-I: Conversion of the digital number (DN) to radiance or converting it to top of atmosphere (TOA) radiance ( $L_k$ ). The thermal band, band 6 of Landsat-7 ETM+ imagery has been utilized to compute the spectral radiance ( $L\lambda$ ) using the following equation.

$$L\lambda = LMIN\lambda \frac{(Lmax\lambda - Lmin\lambda)}{(QCALmax - QCALmin)} \times QCAL \dots \dots \dots (6)$$

where, QCALmax and QCALmin are the maximum and minimum DN values (usually 255 and 1, respectively); QCAL is the Digital Number of each pixel; Lmax $\lambda$  and Lmin $\lambda$  are the spectral radiances for the band 6 at digital number. The value of Lmax $\lambda$  = 17.040 and Lmin $\lambda$  = 0. The thermal band for Landsat-8 OLI imagery is band 10. To calculate the spectral radiance ( $L\lambda$ ), the following equation 7 is used,

$$L\lambda = ML \times (QCAL + AL - Oi) \dots \dots \dots (7)$$

where,  $L\lambda$  is the Spectral Radiance of top of the atmosphere; ML is the band-specific multiplicative rescaling factor (0.0003342); AL is the band-specific additive rescaling factor (0.1); QCAL is the Quantized and Calibrated Standard Product Pixel value (band 10 image); Oi is the Correction for band-10 (0.29).

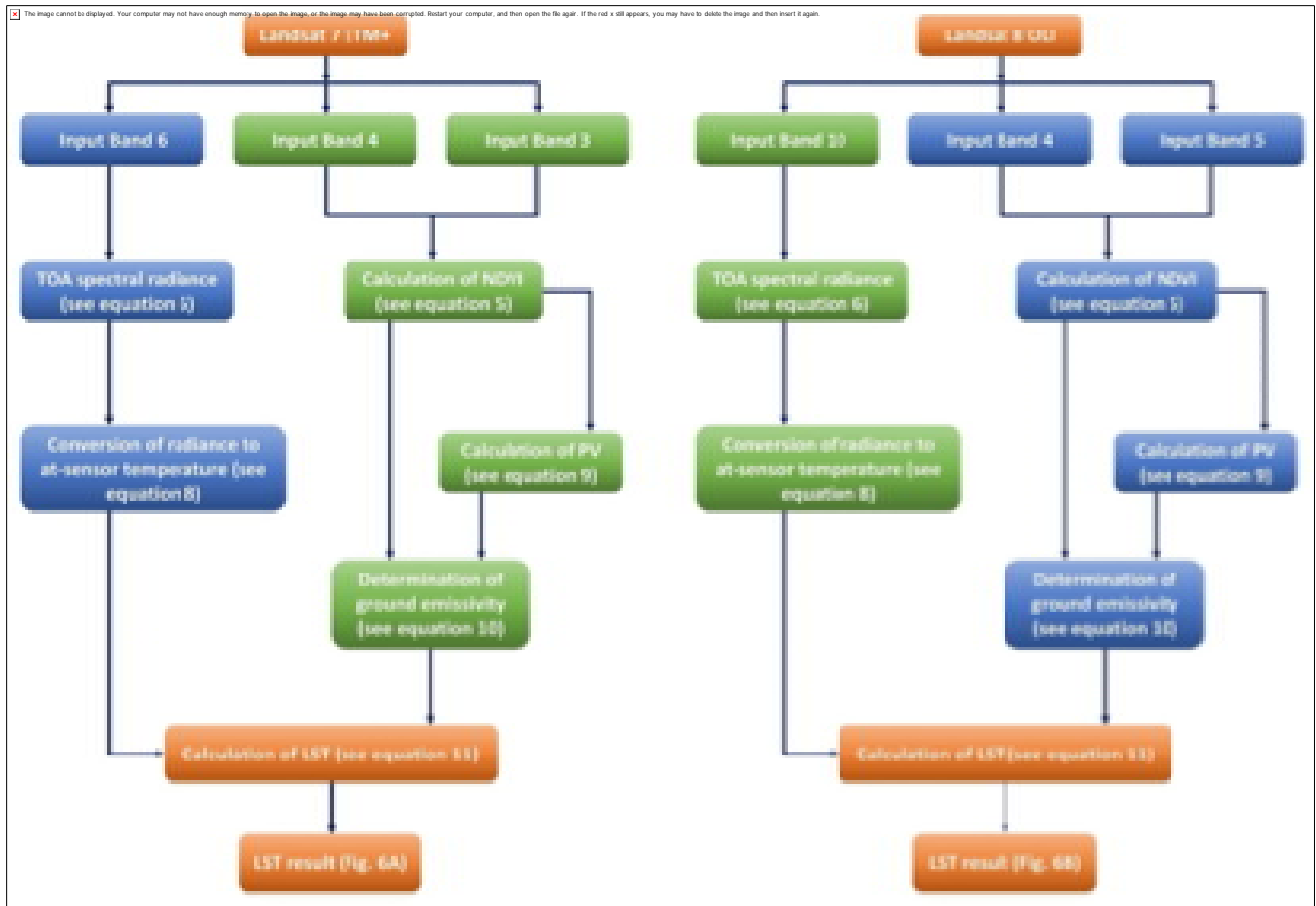


Figure 3 Procedures for LST calculation by using Landsat 7 ETM+ (A) and Landsat 8 OLI (B).

Step-II: Conversion of spectral radiation to satellite-derived brightness temperatures (BT). Upon converting the digital number into radiance, the data has been transformed into brightness temperature (BT) using the thermal constant provided in the metadata file. The tool's algorithm uses the following equation to convert reflectance to BT [equation 8].

$$BT = \left( \frac{K2}{\ln[(K1 / L\lambda) + 1]} \right) - 273.15 \dots \dots \dots (8)$$

where, BT is the satellite-derived brightness temperatures;  $L\lambda$  is the TOA spectral radiance [equation (6)]; K1 is the Band constant (shown in Table 2); K2 is the Band constant 273.15 (shown in Table 2), that helps to convert the temperature from Kelvin to Celsius.

Step III: Calculation of the proportion of vegetation (Pv). The NDVI is the primary metric used to determine the proportion of vegetation. The calculation was performed as follows [equation 9].

$$Pv = \left( \frac{NDVI - NDVImin}{NDVImax - NDVImin} \right)^2 \dots\dots\dots (9)$$

where, NDVI is the Normalized difference vegetation index; NDVImin is the minimum value of NDVI; and NDVImax is the maximum value of NDVI.

Step IV: Emissivity adjustment (ε). The emissivity (ε) can be adjusted by using the equation provided in equation 10.

$$\text{The land surface emissivity } \varepsilon = 0.004 \times PV + 0.986 \dots\dots\dots (10)$$

Step-V: Calculation Land surface temperature (LST).

$$LST = \frac{BT}{[1 + \{(\lambda \times \frac{BT}{\rho}) \times \ln \varepsilon\}]} \dots\dots\dots (11)$$

where, λ is the wavelength of emitted radiance in meters (Markham and Barker, 1985); ρ = h × c / σ, which value is 1.438 × 10<sup>-2</sup> mK; σ is the Boltzmann constant (1.38 × 10<sup>-23</sup> J/K); h is the Planck's constant (6.626 × 10<sup>-34</sup> Js); c is the velocity of light (2.998 × 10<sup>8</sup> m/s); and ε is the emissivity ranging between 0.97 and 0.99.

Table 2 Thermal Constants

Sensor	Year	Band	Band constant K1	Band constant K2
Landsat ETM+	2002	Band 6	666.09	1282.71
Landsat OLI	2022	Band 10	777.8853	1321.0789

### The land use categories

The land uses within the research region were categorized into four unique classifications, such as (i) Water Bodies, (ii) Vegetation, (iii) Build Up Area, (iv) Bare Soil (Table 3). After

categorizing the photos based on the above land use categories, maps were generated with appropriate designs at a scale of 1cm = 5km (Figure 4).

## Result and discussion

### Land cover dynamics in the Jashore District from the year 2002 to 2022

The land use pattern for the year 2002 and 2022, consisting of four categories, is presented in Table 3 and visually shown in Figure 4. The land area of Jashore in 2002 was estimated to be 2545.32 km<sup>2</sup> by supervised image classification using ArcGIS 10.8. The land use classification conducted in 2002 served as the basis for visually interpreting the land use pattern in 2022. The sequence of highest areas of land use in 2002 was vegetation area > bare soil > water bodies > build-up area, whereas the sequence in 2022 was bare soil > build up area > vegetation > water bodies. Out of the four land use categories, two important categories i.e., bare soil and build up area had an increase of 15% and 20%, respectively in the year 2022 compared to the year 2002. In contrast, the areas of vegetation and water bodies decreased of 33% and 3%, respectively, in 2022 (Table 3).

Table 3 LULC change detection of Jashore district based on the time frame 2002-2022

Land type classifications	Description land use feature	Land Use in 2002		Land Use in 2022		Changes of LULC over 20 years		
		Area (km <sup>2</sup> )	Land area (%)	Area (km <sup>2</sup> )	Land area (%)	Changed area (km <sup>2</sup> )	% of change	Annual rate of change (%)
Water Bodies	River, lake and pond	100.12	4	28.16	1	(-) 74.64	(-) 2.93	(-) 3.73
Vegetation	Fruit tree and bush	1347.36	53	520.84	20	(-) 823.89	(-) 32.37	(-) 41.19
Build Up Area	Building area including industry and commercial area	28.64	1	544.48	21	(+) 528.60	(+) 20.77	(+) 26.43
Bare Soil	Riverbank, landfill and barren land	1068.87	42	1451.67	57	(+) 369.93	(+) 14.53	(+) 18.50
Total area		2545.32	100	2545.32	100			

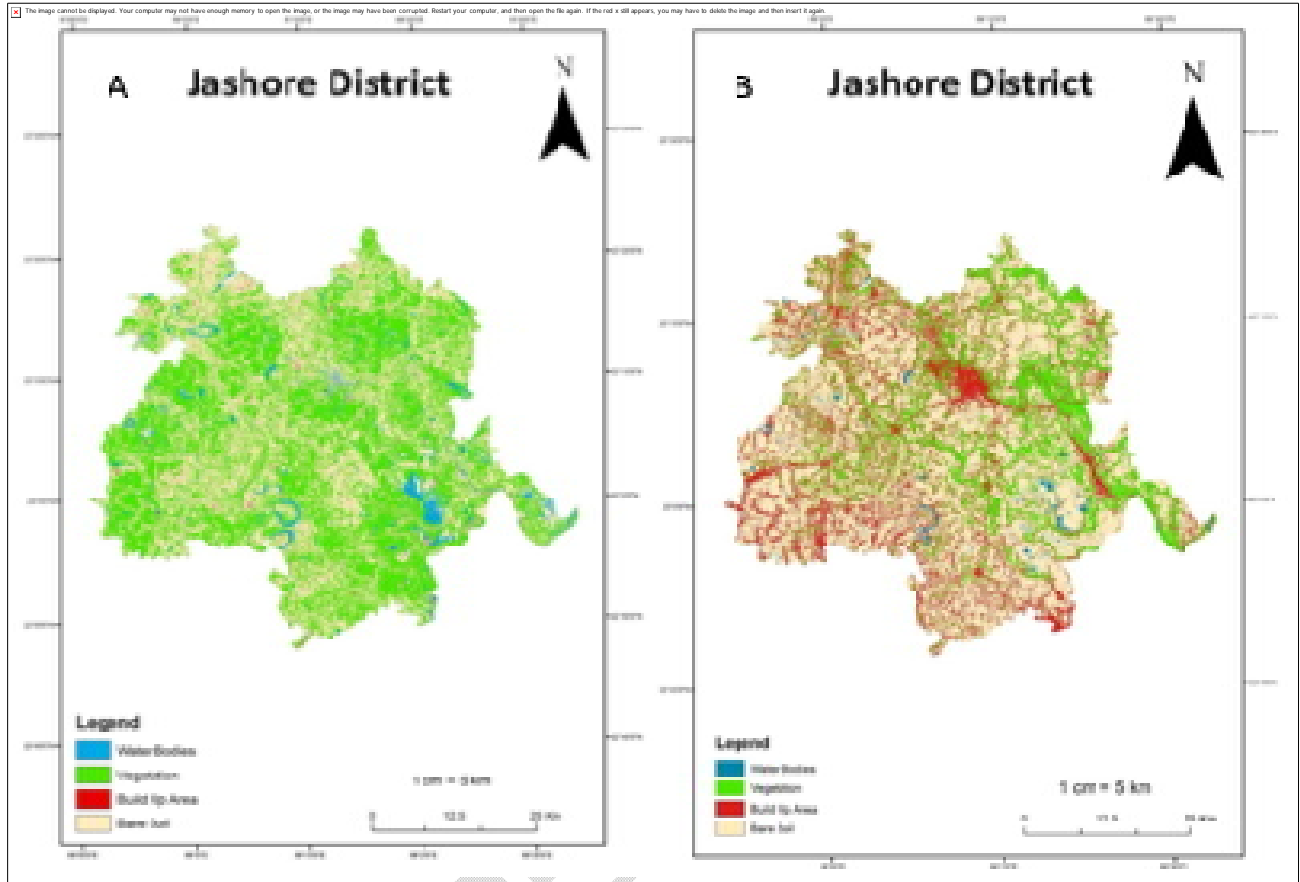


Figure 4 LULC map of Jeshore District in the year 2002 (A) and in the year 2022 (B).

The assessment of the changes in land use categories between 2002 and 2022 revealed a combination of positive and negative changes across different classes, as shown in Table 3. A total of approximately 824km<sup>2</sup> of vegetation area had been reduced between the years 2002 and 2022 with an annual reduction of 41%. The area of water bodies exhibited a decrease of approximately 75 km<sup>2</sup> with a rate of 3.7% annually. During the period from 2002 to 2022, a total of approximately 529 km<sup>2</sup> of land was used for commercial and settlement purpose, with a change rate of approximately 26% annually. Several previous studies of LULC changes also revealed that cropland and waterbody areas in Bangladesh had been declining rapidly (Kafy et al. 2020; Morshed et al. 2021). This study illustrated that, a large area of land cover of forests and

vegetations in the study district has been used for widespread human settlement and development of commercial area over 20 years period. To cope up with population pressure and modernization, urbanization is rapidly changing the LULC across the world during the last few decades (Kafy et al. 2021). The result coincides the future LULC modeling of Jashore city by Morshed et al. (2023), who expected the urban area to be increased by 23.64%, whereas vegetation and water areas to be reduced by 5.47% and 7.73% respectively by the year 2050 compared to 2020. However, the present study revealed an opposite trend in LULC change of bare soil category, as bare soil increased by approximately 15% in 2022 compared to 2002 (Table 3). Morshed et al. (2023) predicted a reduce of bare land by 9.55% by the year 2050 compared to 2020. He also reported that the urban areas would be increasing at the fastest rate during 2020–2030. Our study findings contribute to replan any decision about ecological and environmental development of the bare soil in Jashore District.

### **Evaluation of accuracy and calculation of kappa statistics**

Accuracy assessment is crucial in the analysis of remotely sensed data as it allows for the evaluation of the heterogeneity and validation of the classified images (Elkington 2007). The supervised classification of images yielded different levels of accuracy, which was evaluated by Kappa Statistics, a metric that quantifies the concordance between referred and user-observed categorized data. The results of Kappa coefficient were 0.80 for the 2022 classification and 0.65 for the 2002 classification. Thus, the image taken in 2022 by Landsat OLI (Table 2) had the maximum accuracy of 80%, while the image taken by Landsat ETM+ (Table 2) in 2002 showed the accuracy of 65%. According to Landis and Koch (1977) Kappa coefficient values between 0.61 and 0.80 indicated that the supervised classification had a significant level of

concurrency. The accuracy of a classification is highly dependent on the version of satellite dataset (Haque and Basak 2017). Advanced version of satellite can produce more accurate result.

### **Analysis of NDVI in Jashore District between the years 2002 and 2022**

The measurement of the vegetation area of Jashore District was carried out with the Normalized Difference Vegetation Index (NDVI), classifying measurements into three distinct categories: low, moderate, and high. The value of NDVI ranges from +1 to -1. Values close to +1 indicates denser and greener vegetation, whereas those close to '0' or less represents less green or other colored vegetation or dry leaf. The NDVI value '0' characterizes no vegetation and '0 to 1' means other land cover types (Haque and Basak 2017). In 2002, the NDVI analysis indicated that around 30% of the whole map consisted of areas with low values ranging from -0.06 to -0.15 (Figure 5A). After 20 years, in 2022, the low value -0.06 had risen to 36% as -0.11 (Figure 5B). This indicated a surge in the size of water bodies or areas devoid of vegetation throughout the time. The values close to zero are classified as mixed vegetation which might consist of settlement, water body, or any other land cover feature (Haque and Basak 2017). In 2002, approximately 53% of the land was covered by moderate NDVI values ranging from 0.16 to 0.22 (Figure 5A). Notably, the image taken in 2022 exhibited substantial alterations with moderate values ranging from 0.12 to 0.21 encompassing 30% of the Jashore District (Figure 5B). This indicated a reduction in the amount of moderate vegetation.

In 2002, approximately 17% of the area was covered by high vegetation, identified by NDVI values ranging from 0.23 to 0.39 (Figure 5A). However, in 2022, the high value NDVI of ranged from 0.22 to 0.5 (Figure 5B), which indicated an increase in high vegetation comprised of 34% of the land area. An incline in positive values indicating forested high land vegetation represented a notable increase in plant growth over the span of 20 years. NDVI is the most effective indicator

for categorizing native forests, especially for places with medium to high vegetation density (Piyooosh and Ghosh 2022). Since NDVI is less affected by soil and atmosphere, it might be affected by the vegetation type and growth phase (Muradyan et al. 2019). NDVI is a useful metric to show a significant increase with a clear upwards trend, vegetation and canopy cover (Roy and Bari 2022). Thus, the present finding of the higher NDVI values of denser and greener vegetation area expanding by two times of its original size demonstrated major alterations of land use between 2002 and 2022, which might be due to high growth of planted vegetation with large volume of dense canopy cover. Now a days farmers throughout the country are following high yielding crop variety cultivation with huge number of chemical fertilizers. Bangladesh exhibited a small change in net national tree cover with significantly variable forest types (Islam and Ma 2018).

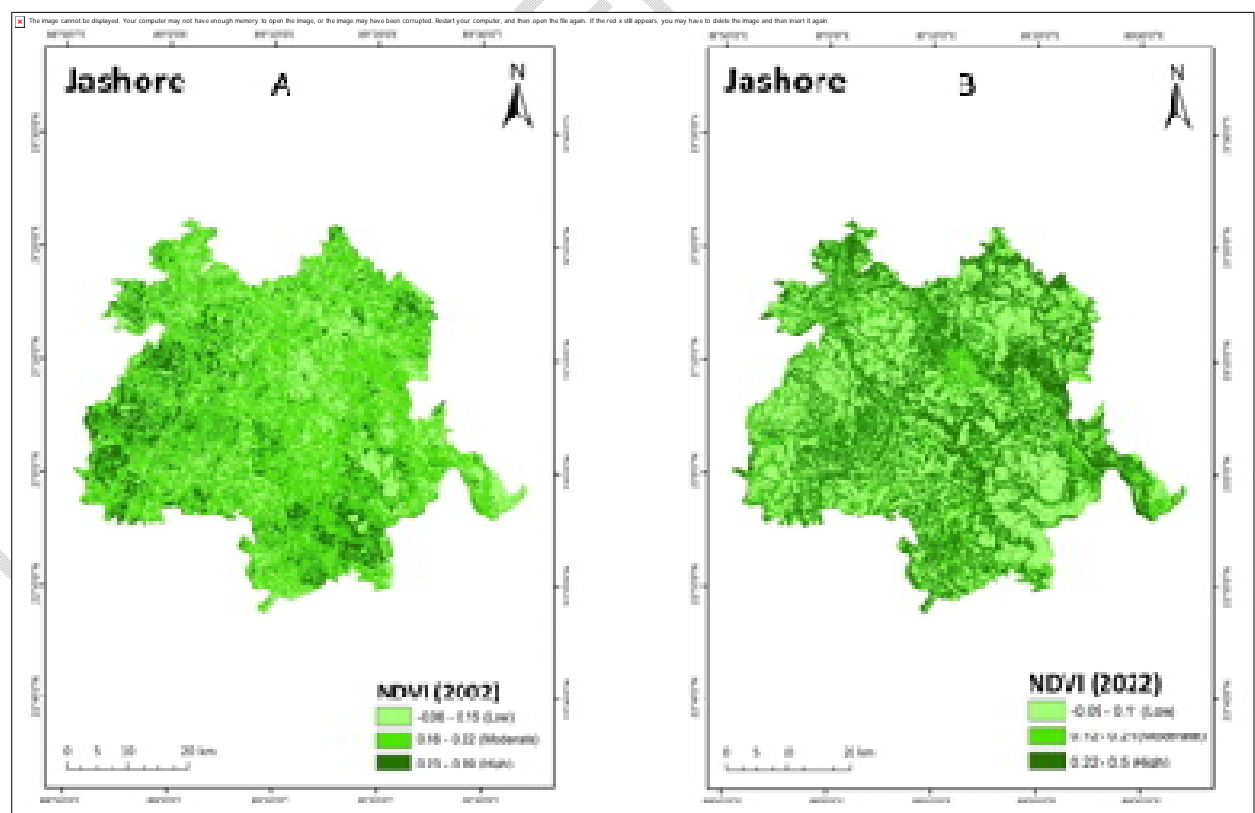


Figure 5. Normalized Difference Vegetation Index (NDVI) of Jashore District in 2002 (A) and IN 2022 (B).

### Changes in land surface temperature (LST)

A significant change in LST in the month of February has been documented within a tenure of 20 years from 2002 to 2022, as presented in Table 4 and Figure 6.

Table 4 LST change over 20 years from 2002 to 2022 in Jashore District, Bangladesh.

Satellite	Land Surface Temperature (LST) in the month of February		
	Minimum Temp. (°C)	Maximum Temp. (°C)	Mean Temp. (°C)
Landsat 2002	20.78	32.18	24.53
Landsat 2022	13.66	23.36	17.24

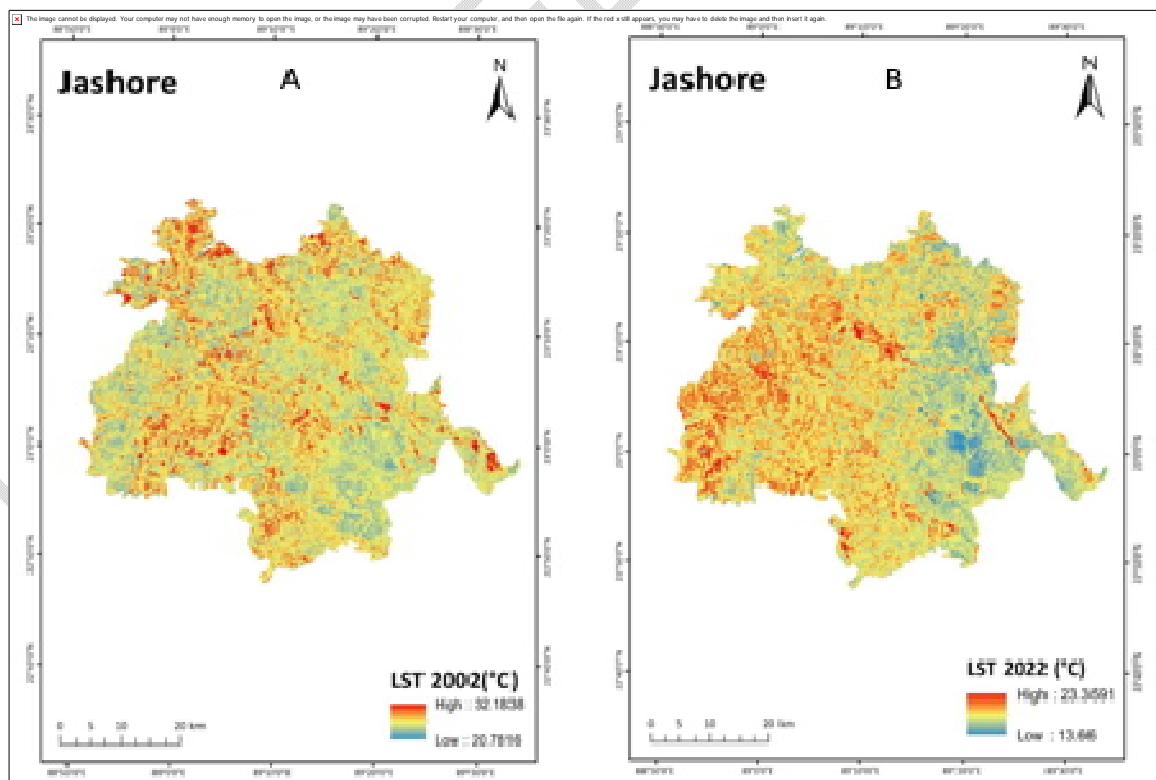


Figure 6. Land surface temperature (LST) showing the minimum and maximum temperature (□) on 7<sup>th</sup> February in 2002 (A) and in 2022 (B).

The trend of LST changes in this investigation signifies a discernible decline in the highest and lowest temperatures over 20 years. Differential composition of urban and rural LULC (Bala et al. 2021; Roy and Bari 2022), natural vegetation cover (Yuan et al. 2017; Bari et al. 2021; Roy 2021), vegetation types (Deng et al. 2018), heat conductivities of urban surfaces, anthropogenic discharges, and density of built-up areas are the contributors to LST intensity (Mathew et al. 2016). Due to the roughness of different LULC and the surface reflectance, the LST of different surface areas varies prominently (Guanglei et al. 2009) in the studied years. Both of the water and vegetation areas contribute negatively to the urban heat island, whereas the built-up areas and barren grounds contribute positively to LST (Bala et al. 2021). However, built-up areas will show greater temperatures than barren grounds since they reflect more heat than the Earth's surface (Aslam et al. 2021). Although LST is a good indicator of heat-retaining or heat-reflecting surfaces, it is also strongly affected by air surface temperature, (Roy and Bari 2022), water body, altitude (Deng et al. 2018) and season (Sun and Kafatos 2007). The decline of the minimum, maximum and mean temperature of land surface in this investigation over a 20-years period (Table 4), associated with a decrease in vegetation and water body areas as well as an increase in build up and bare soil areas, reflected an integrated effects of different land cover types and their characteristics. Different types of vegetation such as woodland, grassland, and cultivated land are shown to affect LST in different ways (Deng et al. 2018; Ismal and Ma 2018). The order of high LST showed by different land use types is construction land > unused land > cultivated land > water body > grassland > woodland/forest land (Deng et al. 2018). To explore

the effects of specific vegetation type on LST might explain better the reason of declining LST in the year 2022 than in 2002.

### Relationship between LST and NDVI

To understand the variations in LST of the study years, whether the vegetation area affected on, the correlation between LST and NDVI was used (Guha and Govil 2021), although the relation might be very complex under the effects of various factors (Deng et al. 2018; Roy and Bari 2022). In a previous study by Deng et al. (2018), the relation between LST and NDVI showed an obtuse-angled triangle shape but a negative linear correlation after excluding the water body data. Sun and Kafatos (2007) found that the correlation between LST and NDVI was negative during warm seasons but positive during the winter. In this study, a negative correlation was observed between NDVI and LST values for both the years 2002 and 2022, as shown in Figure 7.

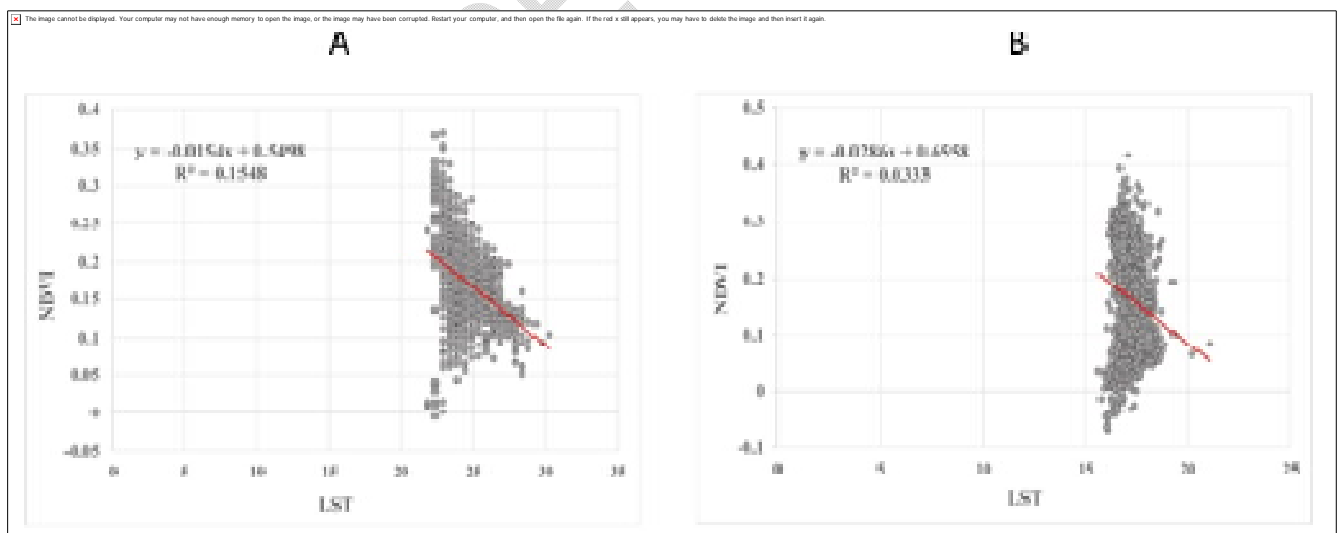


Figure 7. Relationship between LST and NDVI in the years 2002 (A) and 2022 (B).

The correlation between greater LST and lower vegetation densities pointed to a pattern in which warmer climates are linked to less robust or decreased vegetation cover. Additionally, the

regression analysis the data sets showed that the slope of the linear line for the year 2002 is -0.0154 (Figure 7A), which is greater than -0.0286 for the year 2022 (Figure 7B). Thus, a sharper decline of LST values with rising NDVI was observed in 2002 ( $R^2 = 0.1548$ , Figure 7A) than 2022 ( $R^2 = 0.0333$ , Figure 7B). However, for a reduction in one unit of LST required a higher value of NDVI in case of the year 2022 (intercept value is 0.6558; Figure 7B) than the year 2002 (intercept value is 0.5498; Figure 7A). The result might indicate a combined effects of all atmospheric and land type factors influencing the LST, prominently in the recent year 2022.

### **Limitations and future concern**

In this study, recent changes in LULC were considered and estimated by four categories such as water bodies, vegetation, build up area and bare soil, and the relationship between LST and NDVI was analysed to understand the effects of LULC changes on LST. Along with important findings that show remarkable changes in LULC and LST over a period of 20 years in Jashore District in Bangladesh, a robust study including other atmospheric parameters such as air temperature, precipitation, type of vegetation cover, albedo, and soil moisture (Guan et al. 2009; Li et al. 2018; Ismal and Ma 2018) is required. Future studies, including other factors that influence LST, may increase our understanding of the the relationship of LST and vegetation dynamics for concluding the specific effects of LULC on LST and elucidating the relative influence on the other ecological parameters. Such a study is necessary for continuous observation for global trends of urban expansion and environmental modification for ecosystem preservation and reducing the effects of human activity on the environment.

## **Conclusion**

This study provides insightful information about the dynamic changes in land use and land cover in Jashore District of Bangladesh over a period of 20 years from 2002 to 2022 using remote sensing and GIS based data obtained from Landsat satellites. The land use classification analysis showed notable increase in bare soil and built-up areas and decrease in water bodies and vegetation cover. The reliability of the classification process is validated by the accuracy evaluation through the Kappa statistics, which validates the interpretation of land cover patterns. The results are further justified by the application of NDVI analysis, which provides an overall view of vegetation changes. Furthermore, the examination of land surface temperature (LST) has revealed significant temperature changes during the research period mainly due to changes in vegetation types and covered area. The impact of urbanization and changes in land cover, especially vegetation, on regional climate conditions could be justified by the association between LST and NDVI. Findings of this study could be important to Bangladeshi policymakers, urban planners, and environmental conservationists for the development of sustainable land management strategies in the studied area. Continuous studying and monitoring on LULC changes is essential to handle aftereffects of the changes on ecology and environment.

## **Reference**

Agarwal, C., Green, G.M., Grove, J.M., Evans, T.P., and Schweik, C.M. (2001). A Review and Assessment of Land-Use Change Models Dynamics of Space, Time and Human Choice. CIPEC Collaborative Report Series No. 1, Center for the Study of Institutions, Population, and Environmental Change, Indiana University.

- Ahmed, B. (2011). Modelling spatio-temporal urban land cover growth dynamics using remote sensing and GIS techniques: A case study of Khulna City. *Journal of Bangladesh Institute of Planners*, 4, 15–32. [http://www.bip.org.bd/SharingFiles/journal\\_book/20130724135944.pdf](http://www.bip.org.bd/SharingFiles/journal_book/20130724135944.pdf).
- Ahmed, S., and Bramley, G. (2015). How will Dhaka grow spatially in future? -Modelling its urban growth with a near-future planning scenario perspective. *International Journal of Sustainable Built Environment*, 4, 359–377. <http://dx.doi.org/10.1016/j.ijsbe.2015.07.003>.
- Al-Darwish, Y., Ayad, H., Taha, D., and Saadallah, D. (2018). Predicting the future urban growth and its impacts on the surrounding environment using urban simulation models: Case study of Ibb city – Yemen. *Alexandria Engineering Journal*, 57(4), 2887–2895. <https://doi.org/10.1016/j.aej.2017.10.009>.
- Asgarian, A., Amiri, B.J., and Sakieh, Y. (2015). Assessing the effect of green cover spatial patterns on urban land surface temperature using landscape metrics approach. *Urban Ecosystems*, 18, 209-222.
- Aslam, B., Maqsoom, A., Khalid, N., Ullah, F., and Sepasgozar, S. (2021). Urban overheating assessment through prediction of surface temperatures: a case study of karachi, Pakistan. *ISPRS Int. J. Geo-Inf.*, 10(8), 539.
- Audah, S., Rizky, M.M., and Lindawati. (2021). Making of classification land cover through result of visual data satellite image analysis landsat 8 OLI: Case study in Tapaktuan District, South Aceh District. *Jurnal Inotera*, 6(1), 59–65. <https://doi.org/10.31572/inotera.vol6.iss1.2021.id139>

- Bala, R., Prasad, R., and Yadav, V.P. (2021). Quantification of urban heat intensity with land use/land cover changes using Landsat satellite data over urban landscapes. *Theor. Appl. Climatol.*, 145(1–2), 1–12.
- Bari, E., Nipa, N.J., and Roy, B. (2021). Association of vegetation indices with atmospheric and biological factors using MODIS time series products. *Environ. Challenge*, 5, 100376.
- Choudhury, D., Das, K., and Das, A. (2019). Assessment of land use land cover changes and its impact on variations of land surface temperature in Asansol-Durgapur Development Region. *The Egyptian Journal of Remote Sensing and Space Science*, 22(2), 203-218.
- Collins, J.B., and Woodcock, C.E. (1996). An assessment of several linear change detection techniques for mapping forest mortality using multitemporal landsat TM data. *Remote Sensing of Environment*, 56(1), 66–77. [https://doi.org/10.1016/0034-4257\(95\)00233-2](https://doi.org/10.1016/0034-4257(95)00233-2)
- Das, N., Mondal, P., Sutradhar, S., and Ghosh, R. (2021). Assessment of variation of land use/land cover and its impact on land surface temperature of Asansol subdivision. *The Egyptian Journal of Remote Sensing and Space Science*, 24(1), 131-149.
- Deng, Y., Wang, S., Bai, X., Tian, Y., Wu, L., Xiao, J. et al. (2018). Relationship among land surface temperature and LUCC, NDVI in typical karst area. *Sci. Rep.*, 8(1), 641.
- Dewan, A. M., and Yamaguchi, Y. (2009a). Using remote sensing and GIS to detect and monitor land use and land cover change in Dhaka Metropolitan of Bangladesh during 1960– 2005. *Environmental monitoring and assessment*, 150, 237-249.
- Dewan, A. M., and Yamaguchi, Y. (2009b). Land use and land cover change in Greater Dhaka, Bangladesh: Using remote sensing to promote sustainable urbanization. *Applied geography*, 29(3), 390-401.

- Elkington, M.D. (1987). A review of: "Remote Sensing Digital Image Analysis: An Introduction" by J. A. Richards. *International Journal of Remote Sensing*, 8(7), 1075. <https://doi.org/10.1080/01431168708954750>.
- Faisal, A.-A., Kafy, A.-A., Rakib, A.A., et al. (2021). Assessing and predicting land use/land cover, land surface temperature and urban thermal field variance index using Landsat imagery for Dhaka Metropolitan area. *Environ., Chall.* 4, 100192.
- Fan C., Myint, S.W., Kaplan, S., Middel, A., Zeng, B., Rahman, A., et al. (2017). Understanding the impact of urbanization on surface urban heat islands—A longitudinal analysis of the oasis effect in subtropical desert cities. *Remote Sens.*, 9(7), 672, doi: 10.3390/rs9070672.
- Feng, Y., Li, H., Tong, X., Chen, L., and Liu, Y. (2018). Projection of land surface temperature considering the effects of future land change in the Taihu Lake Basin of China. *Glob. Planet. Change*, 167, 24–34. doi: 10.1016/j.gloplacha.2018.05.007.
- Gómez, J., Patiño, J., Duque, J., and Passos, S. (2020). Spatiotemporal modeling of urban growth using machine learning. *Remote Sensing*, 12(1), 109. <https://doi.org/10.3390/rs12010109>
- Gopal, S., and Woodcock, C. 1996. Remote sensing of forest change using artificial neural networks. *IEEE Transactions on Geoscience and Remote Sensing*, 34(2), 398-404.
- Govind, N.R., and Ramesh, H. (2019). The impact of spatiotemporal patterns of land use land cover and land surface temperature on an urban cool island: a case study of Bengaluru. *Environmental monitoring and assessment*, 191, 1-20.
- Grant, U. (2010). Spatial inequality and urban poverty traps. London, UK: Overseas Development Institute. Retrieved from <https://www.odi.org/publications/4526-spatial-inequality-andurban-poverty-traps>

- Guan, X., Huang, J., Guo, N., Bi, J., and Wang, G. (2009). Variability of soil moisture and its relationship with surface albedo and soil thermal parameters over the loess plateau. *Adv. Atmos. Sci.*, 26, 692–700.
- Guanglei, H., Hongyan, Z., Yeqiao, W., Zhihe, Q., and Zhengxiang, Z. (2009). Retrieval and spatial distribution of land surface temperature in the middle part of jilin province based on MODIS data. *Sci. Geogr. Sin.* 30(3), 421–427. Accessed: Aug. 16, 2021. [Online]. Available: [https://en.cnki.com.cn/Article\\_en/CJFDTotol-DLKX201003017.htm](https://en.cnki.com.cn/Article_en/CJFDTotol-DLKX201003017.htm).
- Guha, S., and Govil, H. (2021). An assessment on the relationship between land surface temperature and normalized difference vegetation index. *Environ. Dev. Sustain.*, 23(2), 1944–1963.
- Hassan, M.M. (2017). Monitoring land use/land cover change, urban growth dynamics and landscape pattern analysis in five fastest urbanized cities in Bangladesh. *Remote Sensing Applications: Society and Environment*, 7, 69-83. <https://doi.org/10.1016/j.rsase.2017.07.001>
- Hassan, M.M., and Nazem, M.N.I. (2016). Examination of land use/land cover changes, urban growth dynamics, and environmental sustainability in Chittagong city Bangladesh. *Environ. Dev. Sustain.*, 18, 697–716. <https://doi.org/10.1007/s10668-015-9672-8>.
- Haque, M.I., and Basak, R. (2017). Land cover change detection using GIS and remote sensing techniques: A spatio-temporal study on Tanguar Haor, Sunamganj, Bangladesh. *The Egyptian Journal of Remote Sensing and Space Sciences*, 20, 251–263. <http://dx.doi.org/10.1016/j.ejrs.2016.12.003>
- Hossain, M.S., and Rahman, M. (2022). Assessment of Land Use/Land Cover (LULC) changes and urban growth dynamics using remote sensing in Dhaka City, Bangladesh. In:

- Dissanayake, R., Mendis, P., Weerasekera, K., De Silva, S., Fernando, S. (eds) ICSBE 2020. Lecture Notes in Civil Engineering, vol 174. Springer, Singapore. [https://doi.org/10.1007/978-981-16-4412-2\\_48](https://doi.org/10.1007/978-981-16-4412-2_48).
- Islam, M.S., and Ahmed, R. (2011). Land Use Change Prediction In Dhaka City Using Gis Aided Markov Chain Modeling. *J. Life Earth Sci.*, 6, 81-89. <http://banglajol.info.index.php/JLES>.
- Iqbal, M.F., and Khan, I.A. (2014). Spatiotemporal land use land cover change analysis and erosion risk mapping of Azad Jammu and Kashmir, Pakistan. *Egypt. J. Remote Sens. Space Sci.*, 17, 209– 229. <http://dx.doi.org/10.1016/j.ejrs.2014.09.004>.
- Islam, S., and Ma, M. (2018). Geospatial monitoring of land surface temperature effects on vegetation dynamics in the southeastern region of Bangladesh from 2001 to 2016. *ISPRS Int. J. Geo-Inf.*, 7, 486; doi:10.3390/ijgi7120486
- Kafy, A., Faisal, A., Hasan, M.M., Sikdar, M.S., Khan, M.H.H., Rahman, M., and Islam, R. (2019). Impact of LULC Changes on LST in Rajshahi District of Bangladesh: A Remote Sensing Approach. *J. Geographical Studies*, 3 (1), 11-23. <https://dx.doi.org/10.21523/gcj5.19030102>.
- Kafy, A.-A., Hasan, M.M., Faisal, A.-A., Islam, M., and Rahman, M.S. (2020). Modelling future land use land cover changes and their impacts on land surface temperatures in Rajshahi, Bangladesh. *Remote Sensing Applications: Society and Environment*, 18(2).
- Kafy, A.-A., Faisal, A.-A., Rahman, A.S., Islam, M., Rakib, A.-A., Islam, M.A., et al. (2021). Prediction of seasonal urban thermal field variance index using machine learning algorithms in Cumilla, Bangladesh. *Sustainable Cities and Society*, 64, 102542. <https://doi.org/10.1016/j.scs.2020.102542>.

- Kantakumar, L.N., and Neelamsetti, P. (2015). Multi-temporal land use classification using hybrid approach. *Egypt. J. Remote Sens. Space Sci.*, 18, 289–295. <http://dx.doi.org/10.1016/j.ejrs.2015.09.003>.
- Kumar, K.S., Bhaskar, P.U., and Padmakumari, K. (2012). Estimation of land surface temperature to study urban heat island effect using Landsat ETM+ image. *Int. J. Eng. Sci. Technol.*, 2, 771–778.
- Kumar, D., and Shekhar, S. (2015). Statistical analysis of land surface temperature-vegetation indexes relationship through thermal remote sensing. *Ecotoxicol. Environ. Saf.*, 121, 39–44. doi:10.1016/j.ecoenv.2015.07.004.
- Landis, J.R., and Koch, G.G. (1977). The measurement of observer agreement for categorical data. *Biometrics*, 159–174.
- Li, Q., Ma, M., Wu, X., and Yang, H. (2018). Snow cover and vegetation-induced decrease in global albedo from 2002 to 2016. *J. Geophys. Res. Atmos.*, 123.
- Lin, C., Wu, C.C., Tsogt, K., Ouyang, Y.C., and Chang, C.I. (2015). Effects of atmospheric correction and pan sharpening on LULC classification accuracy using WorldView-2 imagery. *Inf. Process. Agric.*, 2, 25–36. <http://dx.doi.org/10.1016/j.inpa.2015.01.003>.
- López, E., Bocco, G., Mendoza, M., and Duhau, E. (2001). Predicting land-cover and land-use change in the urban fringe. *Landscape and Urban Planning*, 55(4), 271–285. [https://doi.org/10.1016/s0169-2046\(01\)00160-8](https://doi.org/10.1016/s0169-2046(01)00160-8).
- Maarseveen, M., Martinez, J., and Flacke, J. (2018). GIS in sustainable urban planning and management: A global perspective (1st Edn). CRC Press. <https://doi.org/10.1201/9781315146638>

- Mamun, A.A., Mahmood, A., and Rahman, M. (2013). Identification and monitoring the change of land use pattern using remote sensing and GIS: A case study of Dhaka City. *IOSR Journal of Mechanical and Civil Engineering*, 6(2), 20-28.
- Mathew, A., Khandelwal, S., and Kaul, N. (2016). Spatial and temporal variations of urban heat island effect and the effect of percentage impervious surface area and elevation on land surface temperature: study of Chandigarh city, India. *Sustain. Cities Soc.*, 26, 264–277.
- Mishaa, M., Manikandan, A.D., and Neebha, T.M. (2021). Image based land cover classification for remote sensing applications: A review. 2021 3rd International Conference on Signal Processing and Communication (ICPSC). IEEE. <http://dx.doi.org/10.1109/icspc51351.2021.9451755>
- Mondal, M.S., Sharma, N., Garg, P.K., and Kappas, M. (2016). Statistical independence test and validation of CA Markov land use land cover (LULC) prediction results. *Egypt. J. Remote Sens. Space Sci.*, 19 (2), 259–272. <http://dx.doi.org/10.1016/j.ejrs.2016.08.001>.
- Mondal, M.S., and Wasimi, S.A. (2004). Impact of climate change on dry season water demand in the Ganges Delta of Bangladesh. In *Contemporary Environmental Challenges*, 1st ed.; Rahman, M.M., Alam, M.J.B., Ali, M.A., Ali, M., Vairavamoorthy, K., Eds.; CERM and ITN, BUET: Dhaka, Bangladesh; WEDC, IDE, Loughborough University: Loughborough, UK, pp. 63–83.
- Moore, M., Gould, P., and Keary, B. (2003). Global urbanization and impact on health. *International Journal of Hygiene and Environmental Health*, 206(4–5), 269–278. <https://doi.org/10.1078/1438-4639-00223>
- Morshed, S.R., Fattah, M.A., Haque, M.N., and Morshed, S.Y. (2021). Future ecosystem service value modeling with land cover dynamics by using machine learning based Artificial

- Neural Network model for Jashore city, Bangladesh. *Physics and Chemistry of the Earth, Parts a/b/c*. <https://doi.org/10.1016/j.pce.2021.103021>.
- Morshed, S.R., Fattah, M.A., Hoque, M.M., Islam, M.R. Sultana, F., Fatema, K. et al. (2023). Simulating future intra-urban land use patterns of a developing city: a case study of Jashore, Bangladesh. *GeoJournal*, 88, 425–448. <https://doi.org/10.1007/s10708-022-10609-4>
- Muradyan, V., Tepanosyan, G., Asmaryan, S., Saghatelian, A., and Dell'Acqua, F. (2019). Relationships between NDVI and climatic factors in mountain ecosystems: a case study of Armenia. *Remote Sens. Appl. Soc. Environ.*, 14, 158–169. [http://refhub.elsevier.com/S2405-8440\(22\)01956-9/sref63](http://refhub.elsevier.com/S2405-8440(22)01956-9/sref63)
- Pal, S., and Ziaul, S.K. (2017). Detection of land use and land cover change and land surface temperature in English Bazar urban center. *The Egyptian Journal of Remote Sensing and Space Science*, 20(1), 125-145.
- Piyooosh, A.K., and Ghosh, S.K. (2022). Analysis of land use land cover change using a new and existing spectral index and its impact on normalized land surface temperature. *Geocarto Int.*, 37(8), 2137–2159. [http://refhub.elsevier.com/S2405-8440\(22\)01956-9/sref62](http://refhub.elsevier.com/S2405-8440(22)01956-9/sref62)
- Pramanik, M.M.A., and Stathakis, D. (2015). Forecasting urban sprawl in Dhaka city of Bangladesh. *Environment and Planning B: Planning and Design*, 0(0) 1–16. <http://dx.doi.org/10.1177/0265813515595406>
- Rawat, J.S., and Kumar, M. (2015). Monitoring land use/cover change using remote sensing and GIS techniques: A case study of Hawalbagh block, district Almora, Uttarakhand, India. *The Egyptian Journal of Remote Sensing and Space Science*, 18(1), 77-84.

- Roy, B. (2021). A machine learning approach to monitoring and forecasting spatio-temporal dynamics of land cover in Cox's Bazar district, Bangladesh from 2001 to 2019. *Environ. Challenges*, 5, 100237.
- Roy B., and Bari E. (2022). Examining the relationship between land surface temperature and landscape features using spectral indices with Google Earth Engine. *Heliyon* 8, e10668. <https://doi.org/10.1016/j.heliyon.2022.e10668>.
- Salman, M.A., Nomaan, M.S.S., Sayed, S., Saha, A., and Rafiq, M.R. (2021). Land use and land cover change detection by using remote sensing and GIS technology in Barishal District, Bangladesh. *Earth Sciences Malaysia (ESMY)*, 5(1), 33-40. doi: <http://doi.org/10.26480/esmy.01.2021.33.40>.
- Sun, D., and Kafatos, M. (2007). Note on the NDVI-LST relationship and the use of temperature-related drought indices over North America. *Geophysical Research Letters*, 34 (24), L24406. <https://doi.org/10.1029/2007GL031485>.
- Townshend, J.R.G., and Justice, C.O. (1986). Analysis of the dynamics of African vegetation using the normalized difference vegetation index. *International Journal of Remote Sensing*, 7(11), 1435–1445. <https://doi.org/10.1080/01431168608948946>.
- Uddin, K., and Gurung, D. (2008). Land cover change in Bangladesh- a knowledge-based classification approach. In Proceedings of the 10th International Symposium on High Mountain Remote Sensing Cartography ICIMOD, Kathmandu, Nepal, 8–11 September; 41–46.
- Vescovi, F.D., Park, S.J., and Vlek, P.L. (2002). Detection of human-induced land cover changes in a savannah landscape in Ghana: I. Change detection and quantification. 2nd Workshop

of the EARSeL Special Interest Group on Remote Sensing for Developing Countries, Bonn, Germany.

Weng, Q., Lu, D., and Schubring, J. (2004). Estimation of land surface temperature–vegetation abundance relationship for urban heat island studies. *Remote Sensing of Environment*, 89(4), 467-483.

Xu, X., Shrestha, S., Gilani, H., Gumma, M.K., Siddiqui, B.N., and Jain, A.K. (2020). Dynamics and drivers of land use and land cover changes in Bangladesh. *Regional Environmental Change*, 20, 54. <https://doi.org/10.1007/s10113-020-01650-5>

Yuan, F., and Bauer, M.E. (2007). Comparison of impervious surface area and normalized difference vegetation index as indicators of surface urban heat island effects in Landsat imagery. *Int. J. Remote Sens. Environ.*, 106, 375–386.

Yuan, X., Wang, W., Cui, J., Meng, F., Kurban, A., and De Maeyer, P. (2017). Vegetation changes and land surface feedbacks drive shifts in local temperatures over Central Asia. *Sci. Rep.*, 7(1), 3287.